

Supplementary Information

Enhanced photothermal performance of copper nanoparticle-loaded graphene oxide networks for integrated solar-driven water evaporation and energy conversion

Sudeshna Saha^{a,b}, Amarnath Marimuthu^c, Ranita Basu^{b,d}, Manpreet K.T. Bassan^a, Hirakendu Basu^{a,b,*}

^a Analytical Chemistry Division, Bhabha Atomic Research Centre, Trombay, Mumbai-400085, India

^b Homi Bhabha National Institute, Anushaktinagar, Mumbai-400094, India

^c Plasma Research Lab, The Bombay Textile Research Association, Ghatkopar, Mumbai- 400086, India

^d Technical Physics Division, Bhabha Atomic Research Centre, Trombay, Mumbai-400085, India

*Corresponding Author: Email: hirak@barc.gov.in; Tel:91-22-69290312; Fax:91-22-25595151

Chemicals used

Graphite flakes, sulfuric acid, ortho phosphoric acid, potassium permanganate, hydrogen peroxide, hydrochloric acid, copper sulfate, ammonia solution, sodium hydroxide, hydrazine hydrate were purchased from Sisco Research Laboratories Private Limited and Advent Chembio Private Limited.

Instrumentation

For the optical studies, absorption spectra within 200-700 nm were obtained using a Lab India Analytical Instruments UV-Vis spectrophotometer (model UV 3200). Powder X-ray diffraction was carried out with a PROTO AXRD Benchtop diffractometer equipped with a CuK α radiation source ($\lambda = 1.5418 \text{ \AA}$) to evaluate crystal structure and phase composition. Functional group identification and bond analysis were achieved by Fourier-transform infrared spectroscopy using the Bruker Alpha II system. Irradiation experiments were conducted under simulated solar light. A G2V Optics Inc. PICO solar simulator was used for routine illumination, while prolonged irradiation tests employed an Advantech solar simulator fitted with a 200 W Xe lamp. For measurement of intensity of the simulated solar radiation a Lux meter HTC LX101A was used (0- 200,000 Lux with accuracy of $\pm 5\%$ of the reading of $\pm 10\%$ of full scale using silicon photoelectric diode sensor with an optical filter to approximate human eye response). Real-time thermal variations during irradiation were captured with a Thermey 256A infrared imaging camera. Scanning Electron Microscopy images were recorded on an Oxford Instruments Tescan Vega 3, operating at 20 kV with 1.4 nm resolution. For thermal evaporation experiments, water mass loss was monitored using a Wensar Class 1 balance, while

photothermal temperature rise and water evaporation studies were conducted with an in-house fabricated evaporator setup. Major metal ion concentrations in the samples were determined using an Inductively Coupled Plasma–Optical Emission Spectrometer (ICP–OES; Horiba

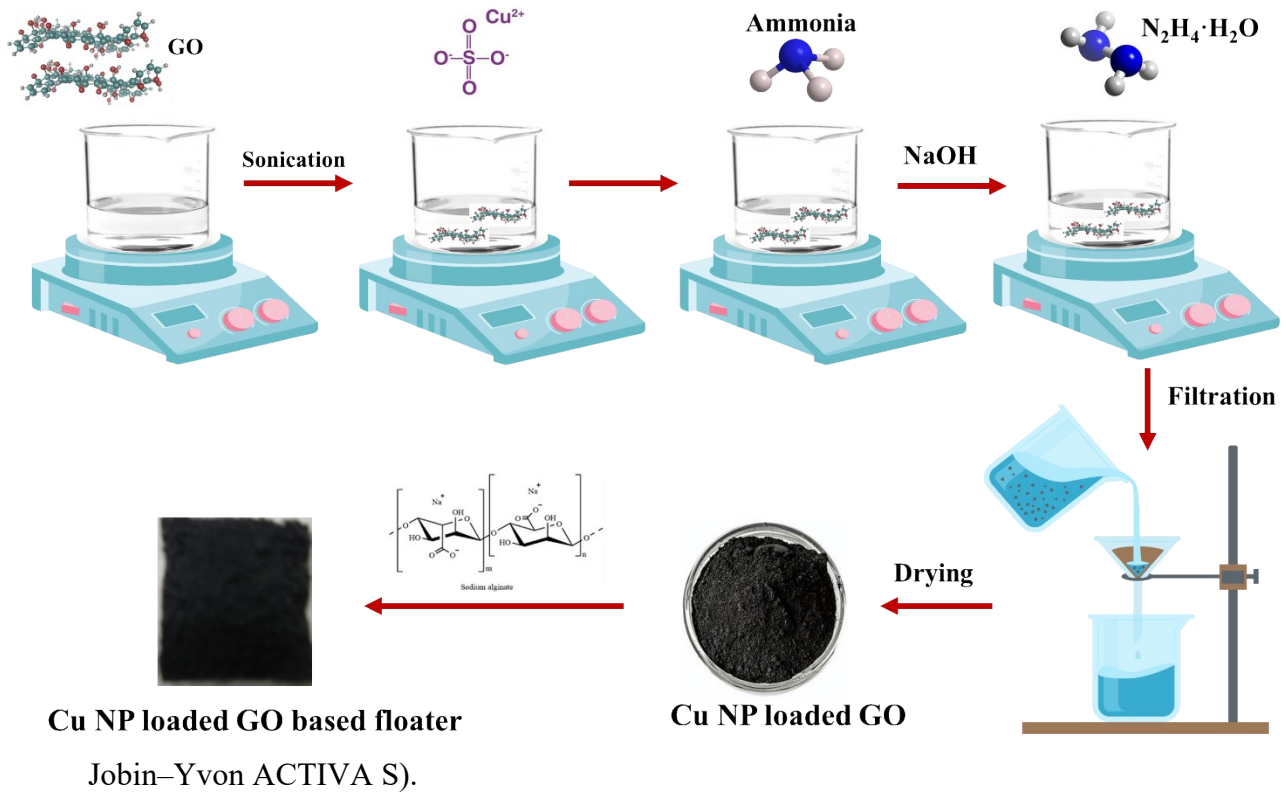


Figure S1: Preparation diagram Cu NP loaded GO based photothermal floater

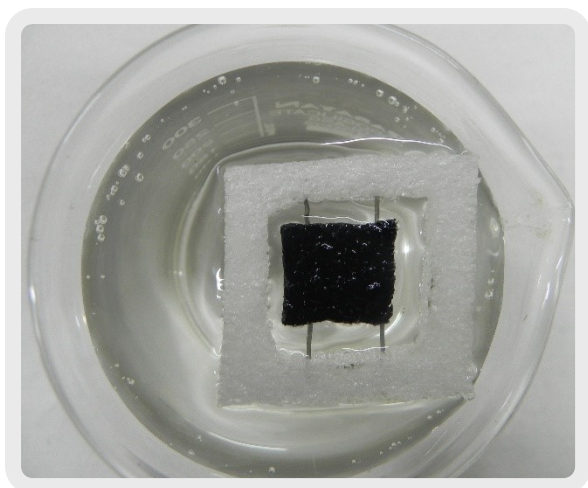


Figure S2: Floater image



Figure S3: Outdoor evaporation set up

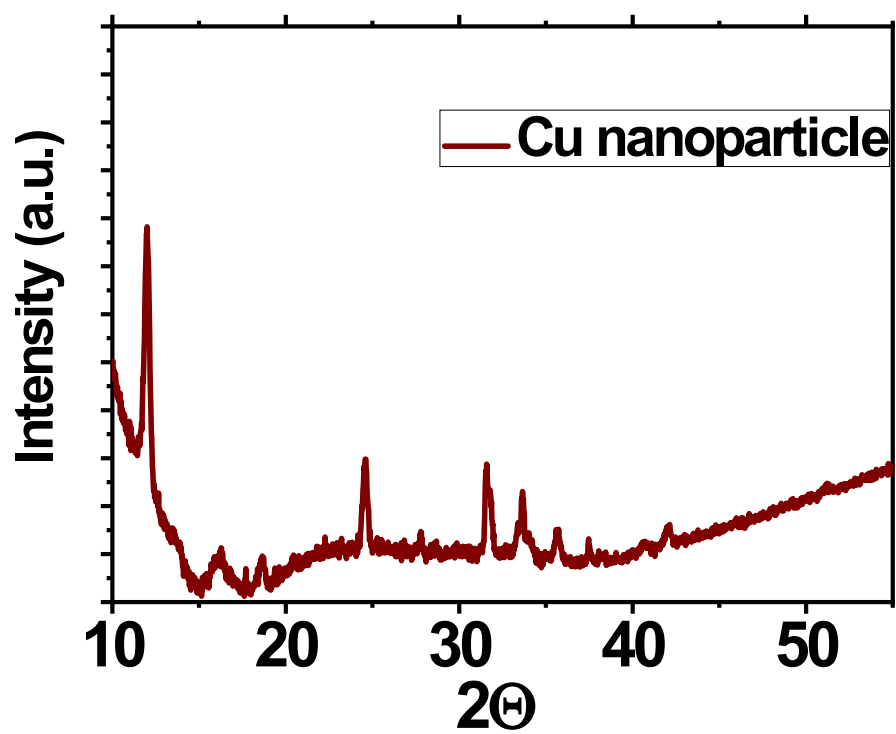


Figure S4: XRD of Cu NP

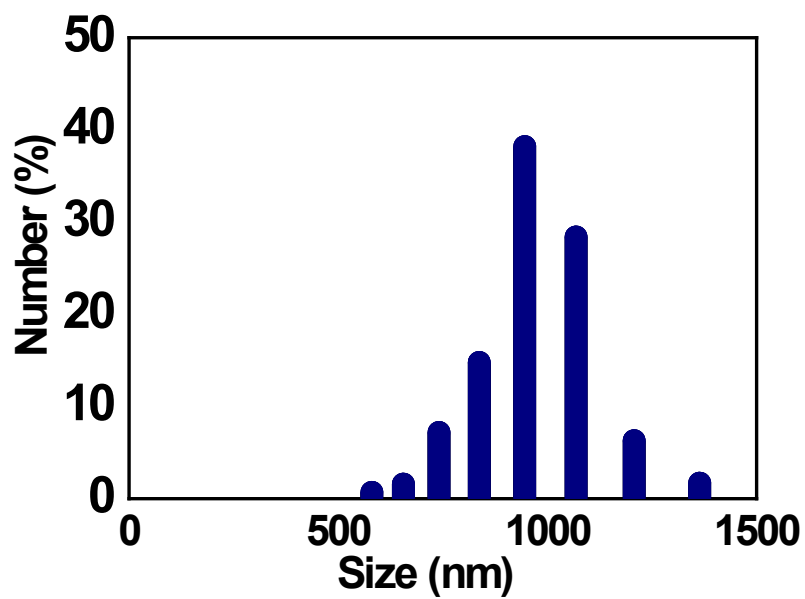


Figure S5: Size distribution of Cu NP

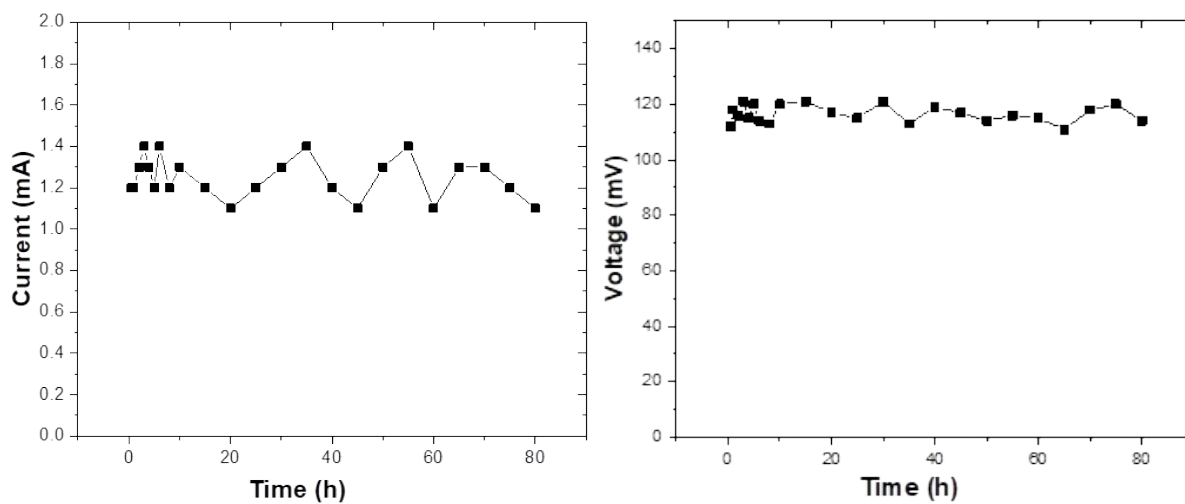
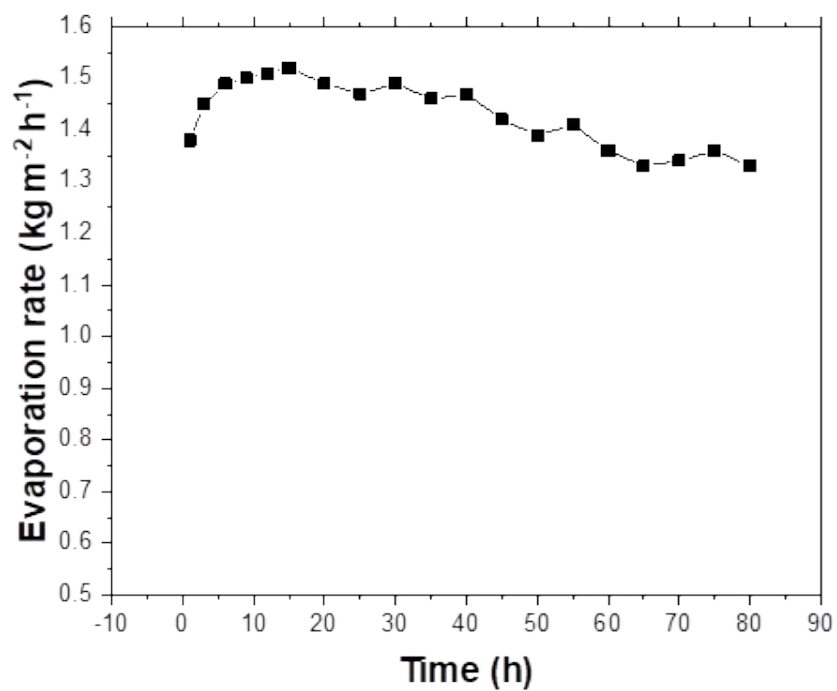


Figure S6: Time-resolved plots of current and voltage recorded over a period of 80h of uninterrupted illumination



Figure

S7: Time-resolved plots of evaporation rate recorded over a period of 80h

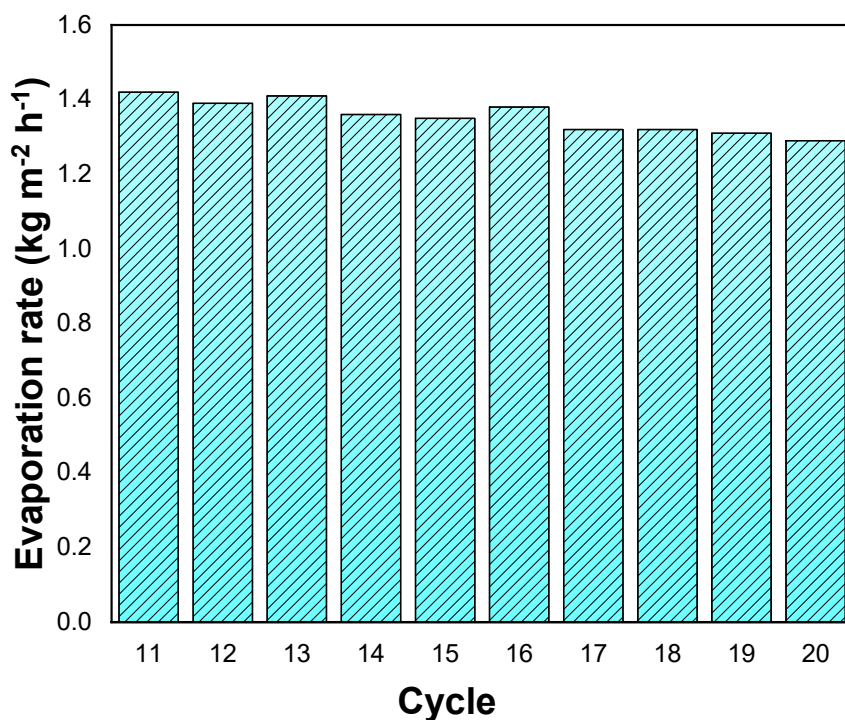


Figure S8: Evaporation rates continuous evaporation cycles 11 to 20 using GO-Cu (1:3) [with reference to Fig. 7 (c)]

Table S1. Comparison of reported works on Cu- and plasmonic NP-based nanocomposites for photothermal applications.

Photothermal Material	Light illumination intensity	Evaporation rate in Kg m ⁻¹ h ⁻¹	Energy conversion efficiency (%)	Harnessed Open circuit voltage (mV)	Reference
Cu-BTC	1 sun	1.13	81.8	-	27
Ag/CuO-rGO	1 sun	2.60	92.5	-	28
CuCN/PDMS@MF	1 sun	1.24	84.9	-	29
Cu@CuO/Cu ₂ O	1 sun	1.53	96.6	-	30
Ag-Cu	1 sun	1.89	90.2	17.3	31
Copper-GO	1 sun	1.25	88.9	-	32
GO-Au	1 sun	1.97	96.7	54.7	33
PTG@CF	1 sun	1.88	88.4	-	34
Polyurethane/Au/Ag	1 sun	1.00	63	-	35
GO/CuO	1 sun	1.71	99.2	-	36
PVA-SA-CNC/PU	1 sun	1.99	89.4	-	37
GO-Cu (1:3)	1 sun	1.6	94	110	This work

The energy conversion efficiency (η) calculation

The efficiency of water evaporation in the photothermal materials was determined by tracking water mass variations under continuous light illumination. Using Eqn. (S1), the efficiency of converting light into heat was quantified

$$\eta = \frac{\frac{dm}{dt} \times S \times H_e}{Q_s} \times 100 \% \quad \text{--- (S1)}$$

Where, $\frac{dm}{dt}$ represents the evaporation rate, H_e is the heat of water evaporation (2260 kJ kg^{-1}), Q_s is the light source's power density (1000 W m^{-2}), m is the mass of evaporated water, t is duration, and S is surface area of the exposed part (effective illuminated surface area).

The evaporation rate was obtained by monitoring the water mass change as a function of time under steady illumination. To reduce environmental contributions, baseline evaporation measured under dark conditions was subtracted. Owing to the interfacial heating configuration, the contribution of sensible heat from bulk water was minimized and therefore not explicitly included in the efficiency estimation. Heat losses due to radiation, convection, and conduction were not separately quantified and are implicitly reflected in the measured evaporation rate. The reported efficiency value should therefore be understood as an estimated photothermal conversion efficiency under the specific experimental conditions employed, rather than an absolute thermodynamic limit.